Korean J. Chem. Eng., **26**(1), 7-13 (2009)

Modeling and control of the melt index in HDPE process

A Ram Seong, Eun Ho Lee, Kyung Nam Lee, and Yeong Koo Yeo†

Department of Chemical Engineering, Hanyang University, Seoul 133-791, Korea
(*Received 10 April 2008 • accepted 22 July 2008*)

Abstract−We investigate the model for an industrial isothermal HDPE slurry reactor. The model, consisting of several nonlinear equations, can be linearized to give sets of linear time invariant state space model. The effectiveness of the linearized model is verified by the numerical simulations. A simple model predictive control scheme is constructed based on the linear state space model. The value of the melt index is obtained from the values of the manipulated and controlled variables generated from the control scheme. The control performance can be evaluated from the comparison between the computed melt index values and measured melt index values. The control scheme shows good tracking performance in the numerical simulations. We believe that the model developed in the present study can be effectively used to predict process variables as well as to control the melt index.

Key words: Model Predictive Control, HDPE, Modeling and Simulation, Melt Index, Grade Change

INTRODUCTION

Demands for high quality and low price are increasing in modern high density polyethylene (HDPE) markets. To meet these demands more precise control operations in the production of HDPE products are requested. In the HDPE production operation the melt index (MI) is by far the most important variable, but it takes a long time to determine the MI experimentally. On-line measurement of the MI is also very difficult because it takes long for the grade to be stabilized during the grade change operation. Moreover, a large amount of off-specification products and significant overshoots arise during the grade change operations. Many computational methods for the MI have been presented, but the effective MI control during the grade change operations is still a challenging problem. In actual operations the MI is controlled by adjusting the amount of hydrogen and ethylene upon which the MI is dependent.

To achieve the on-line evaluation of the MI, McAuley and MacGregor [1-3] proposed an MI estimation method which consists of a log function of the linear combination of the flow rate of each component. Later, Ogawa et al. [4] extended their estimation method by adding a temperature term. But these MI estimation methods require impractical measurements of concentrations of components in the polymerization reactor. Estimation of the concentrations in the polymerization reactor by using only input data would be most helpful for the on-line estimation of the MI as well as the MI control. Use of a suitable process model is imperative to achieve both the correct estimation and control of the MI. Determination of the optimal input data is an additional benefit that can be obtained from the process model. In the present study, we first develop a mathematical model for the production of HDPE and then employ the model to construct a model predictive control (MPC) scheme for the control of the MI in the grade change operations.

1. Process Description

The polymerization reactor shown in Fig. 1 is a batch reactor equipped with a dip tube. The polymerization reaction occurs in the reactor with a volume of 100 m^3 and equipped with an agitator operating with 84 rpm. In typical operations the slurry occupies 90-95% of the reactor volume. The polyethylene slurry is transported to the post reactor by the polymerization pressure which also adjusts the reactor level. The reactor level is measured by the radiation level sensor. Ethylene, comonomer (1-buteme or higher alpha-olefin), hydrogen, catalyst and hexane are fed into the reactor as the reactants.

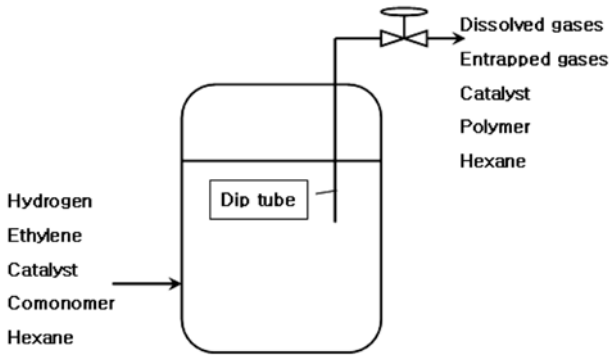

Fig. 1. A schematic of the HDPE reactor considered in the present study.

The normal operating pressure of the reactor is 8-11 atm. The solubility of ethylene and hydrogen increases according to the increase of the operating pressure, which in turn causes the increase of the polymerization rate. The reaction temperature depends upon the product grade. Variations in the reaction temperature adversely affect the MI of the product. Because of this, isothermal operations are preferred in the actual operations. In the process considered in the present study, the isothermal condition is maintained by the cooling system outside the reactor.

It is usual practice for the polymerization reactor to have two outlets because a gas phase and liquid phase exist in the reactor. But the reactor considered in the present study has only one outlet. One of the advantages with a one outlet reactor is the convenience of

†To whom correspondence should be addressed.
E-mail: ykyeo@hanyang.ac.kr

the control of transportation operation from the reactor. Moreover, the level control operation is much more convenient with one outlet when the operating pressure is maintained constant.

The dip tube is always positioned below the slurry level as shown in Fig. 1, and the output from the reactor is transported through the dip tube by the pressure difference. To maintain a constant pressure the valve opening is adjusted. For example, when the reaction pressure is higher than the set point, the valve opening is increased to increase the outflow rate.

2. Process Model

The modeling equations consist of differential algebraic equations (DAEs). If we assume isothermal operations, the amounts of dissolved ethylene and hydrogen are obtained from Henry's law. Eq. (1) represents the behavior of reaction components in the polymerization reactor.

$$\begin{aligned}
\frac{dx_1}{dt} &= F_1 - L_1 - r_1 \\
\frac{dx_2}{dt} &= F_2 - L_2 - r_2 \\
\frac{dx_3}{dt} &= F_3 - L_3 \\
\frac{dx_4}{dt} &= F_4 - L_4 + \frac{28r_2}{1000} \\
\frac{dx_5}{dt} &= F_5 - L_5
\end{aligned} \tag{1}$$

In the above equations F and L denote the feed flow rate and the slurry phase flow, respectively. x_1 and x_2 are the total amount of hydrogen and ethylene, respectively, and x_3, x_4 and x_5 are the amounts of catalyst, comonomer (1-buteme or higher alpha-olefin) and hexane, respectively, in the slurry phase.

The component mass balances in the slurry phase can be written as follows:

$$\frac{ML_1}{(x_4/\rho)+x_5} = \frac{L_1}{(L_4/\rho)+L_5} \tag{2}$$

$$\frac{ML_2}{(x_4/\rho)+x_5} = \frac{L_2}{(L_4/\rho)+L_5} \tag{3}$$

$$\frac{x_3}{(x_4/\rho)+x_5} = \frac{L_3}{(L_4/\rho)+L_5} \tag{4}$$

$$\frac{x_4}{(x_4/\rho)+x_5} = \frac{L_4}{(L_4/\rho)+L_5} \tag{5}$$

where ML denotes the slurry phase. As before, the subscripts 1 and 2 denote hydrogen and ethylene, respectively, in the slurry phase. In the actual operation the volumetric flow rates of catalysts and dissolved gases are much smaller than those of hexane and comonomer. For this reason we assume that the volumetric flow rates of catalysts and dissolved gases are negligible compared to the total flow rate. Then the total flow rate can be represented as the sum of the volumetric flow rates of hexane and comonomer:

$$\frac{L_4}{\rho} + L_5 = 0.2268 C_v \sqrt{\frac{P - P_{out}}{g}} \tag{6}$$

where P represents the reaction pressure (psia) and C_v is the function of the degree of valve opening and is given in Table 1. In the present study C_v was calculated based on the opening of 90° which means fully opened valve. From Eqs. (2)-(5), we have

$$L_2 = L_1\frac{ML_2}{ML_1},\ L_3 = L_1\frac{x_3}{ML_1},\ L_4 = L_1\frac{x_4}{ML_1} \tag{7}$$

The density of the mixture is given by

$$\frac{1}{g} = \frac{x_4}{\rho_4(x_4+\rho_5 x_5)} + \frac{x_5}{x_4+\rho_5 x_5} \tag{8}$$

From Eqs. (6) and (8), we have

$$L_5 = 0.2268 C_v * \sqrt{(P - P_{out})\left(\frac{x_4}{\rho_4(x_4+\rho_5 x_5)} + \frac{x_5}{x_4+\rho_5 x_5}\right)} - \frac{L_4}{\rho_4} \tag{9}$$

By using Henry's law we can get

$$\frac{\alpha_1 MG_1}{(MG_1+MG_2)RT/P} = \frac{x_1}{(x_4/\rho)+x_5} \tag{10}$$

$$\frac{\eta\alpha_2 MG_2}{(MG_1+MG_2)RT/P} = \frac{x_2}{(x_4/\rho)+x_5} \tag{11}$$

where MG denotes the gas phase. The solubility efficiency η is defined as

$$\eta = \frac{1}{(K_p x_3/kL_a x_5)+1} \tag{12}$$

If we assume that the dissolved amount of ethylene is much smaller than the equilibrium value, the total volume can be represented as the sum of the gas volume and the slurry volume:

$$(MG_1+MG_2)\frac{RT}{P} + \frac{x_4}{\rho} + x_5 = V \tag{13}$$

or

$$\text{slurry volume} = Sh = V - MG\frac{RT}{P} \tag{14}$$

From Eqs. (13) and (14), we have

$$Sh = \frac{x_4}{\rho_4} + x_5 \tag{15}$$

Since $x_1=MG_1+ML_1$ and $x_2=MG_2+ML_2$, we get

$$ML_1 = x_1 - MG_1,\ ML_2 = x_2 - MG_2 \tag{16}$$

Table 1. Parameters used in the simulations

Parameter	Value	Reference
T	83 °C	
Controller gain		
Valve bias	90°	Typical value used in the plant
Density of Haxane	0.65	
Density of comonomer	0.62	
V	100 m^3	
A	0.00944	
α_1	0.33	
α_2	3.10	
kL_a	42.50	Kannan et al. [5]
K_p	90	

Values of MG_1 and MG_2 can be obtained from the ideal gas law by assuming that they are ideal gases. Kannan et al. [5] showed that the reaction rates can be given by

$$r_1=\frac{K_pAML_1x_3}{x_5}=\frac{K_pA(x_1-MG_1)x_3}{x_5} \tag{17}$$

$$r_2=\frac{K_pML_2x_3}{x_5}=\frac{K_p\alpha_2Shx_2x_3}{x_5\left\{\alpha_2Sh-(V+Sh)\left(\frac{K_px_3}{kL_ax_5}+1\right)\right\}} \tag{18}$$

For L_1, L_2, L_3, L_4 and L_5, we have

$$L_1=\frac{\alpha_1MG_1Sh}{V-Sh} \tag{19}$$

$$L_2=0.2268C_v\frac{\alpha_2x_2}{Sh\alpha_2+(V-Sh)\left(\frac{K_px_3}{kL_ax_5}+1\right)}*\sqrt{(P-P_{out})\left(\frac{x_4}{\rho_4(x_4+\rho_5x_5)}+\frac{x_5}{x_4+\rho_5x_5}\right)} \tag{20}$$

$$L_3=0.2268C_v\frac{x_3}{Sh}*\sqrt{(P-P_{out})\left(\frac{x_4}{\rho_4(x_4+\rho_5x_5)}+\frac{x_5}{x_4+\rho_5x_5}\right)} \tag{21}$$

$$L_4=0.2268C_v\frac{x_4}{Sh}*\sqrt{(P-P_{out})\left(\frac{x_4}{\rho_4(x_4+\rho_5x_5)}+\frac{x_5}{x_4+\rho_5x_5}\right)} \tag{22}$$

$$L_5=0.2268C_v*\sqrt{(P-P_{out})\left(\frac{x_4}{\rho_4(x_4+\rho_5x_5)}+\frac{x_5}{x_4+\rho_5x_5}\right)}*\left(\frac{x_4/\rho_4+x_5}{x_4}-\frac{1}{\rho_4}\right) \tag{23}$$

Substitution of Eqs. (17), (18) and (20)-(23) into Eq. (1) gives the final modeling equations as follows:

$$\frac{dx_1}{dt}=F_1-\frac{\alpha_1MG_1Sh}{V-Sh}-\frac{K_pA(x_1-MG_1)x_3}{x_5} \tag{24}$$

$$\frac{dx_2}{dt}=F_2-0.2268C_v\frac{\alpha_2x_2}{Sh\alpha_2+(V-Sh)\left(\frac{K_px_3}{kL_ax_5}+1\right)}*\sqrt{(P-P_{out})\left(\frac{x_4}{\rho_4(x_4+\rho_5x_5)}+\frac{x_5}{x_4+\rho_5x_5}\right)}-\frac{K_pSh\alpha_2x_2x_3}{x_5\left(Sh\alpha_2-(V-Sh)\left(\frac{K_px_3}{kL_ax_5}+1\right)\right)} \tag{25}$$

$$\frac{dx_3}{dt}=F_3-0.2268C_v\frac{x_3}{Sh}*\sqrt{(P-P_{out})\left(\frac{x_4}{\rho_4(x_4+\rho_5x_5)}+\frac{x_5}{x_4+\rho_5x_5}\right)} \tag{26}$$

$$\frac{dx_4}{dt}=F_4-0.2268C_v\frac{x_4}{Sh}*\sqrt{(P-P_{out})\left(\frac{x_4}{\rho_4(x_4+\rho_5x_5)}+\frac{x_5}{x_4+\rho_5x_5}\right)}+\frac{56}{1000}\frac{K_px_3}{x_5}\frac{\alpha_2Shx_2}{\alpha_2Sh-(V-Sh)\left(\frac{K_px_3}{kL_ax_5}+1\right)} \tag{27}$$

$$\frac{dx_5}{dt}=F_5-0.2268C_v*\sqrt{(P-P_{out})\left(\frac{x_4}{\rho_4(x_4+\rho_5x_5)}+\frac{x_5}{x_4+\rho_5x_5}\right)}*\left(\frac{x_4/\rho_4+x_5}{x_4}-\frac{1}{\rho_4}\right) \tag{28}$$

The process model depicted as Eqs. (24)-(28) consists of typical nonlinear equations and cannot be used in the MI control operation in this form. Linearization of the model is shown in the Appendix.

3. Control of MI Based on the Linearized Model

In the process model we can see that there are three independent variables and two dependent variables. Table 2 shows a summary of input and output variables. The nonlinear process model obtained above can hardly be used in control, and linearization of the model, as shown in the Appendix, makes it possible to use powerful control techniques such as model predictive control schemes. A time-invariant linear system is represented as

$$\frac{dx}{dt}=Ax+Bu$$
$$y=Cx \tag{29}$$

From the modal transformation we have

$$\frac{d\tilde{x}}{dt}=\tilde{A}\tilde{x}+\tilde{B}\tilde{u}$$
$$y=\tilde{C}\tilde{x} \tag{30}$$

where

$$\tilde{A}=T^{-1}AT$$
$$\tilde{B}=T^{-1}B$$
$$\tilde{C}=CT \tag{31}$$

In the modal transformation, the transformation matrix T is given by $T=[v_1\ v_2\ \dots\ v_n]$ where $v_1, v_2, \dots v_n$ are the eigenvectors of A. From the definition of modal transformation, it is obvious that

$$\tilde{A}=T^{-1}AT=\begin{bmatrix}\lambda_1 & 0 & \dots & 0\\ 0 & \lambda_2 & \dots & 0\\ & \dots\dots\dots & & \\ 0 & \dots & & \lambda_n\end{bmatrix} \tag{32}$$

The linearized process model given in the form of Eq. (30) can be

Table 2. Summary of input and output data

Input data	Output data
MV1: Flow-rate of hydrogen in feed (kmol/h)	MO1: Amount of hydrogen in reactor (kmol)
MV2: Flow-rate of ethylene in feed (kmol/h)	MO2: Amount of ethylene in reactor (kmol)
MV3: Flow-rate of catalyst in feed (mol/h)	
MV4: Flow-rate of hexane in feed (m^3/h)	
MV5: Flow-rate of PRL/BUE in feed (t/h)	

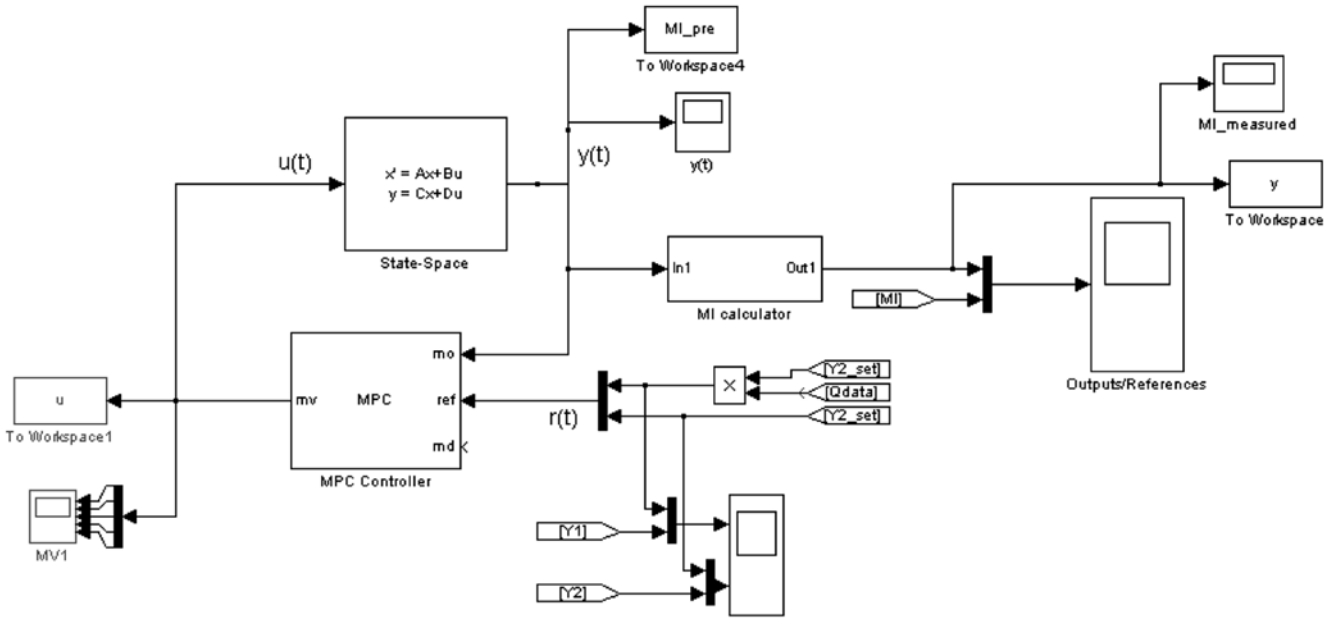

Fig. 2. Configuration of the proposed control system.

effectively used in the construction of a predictive control scheme as shown in Fig. 2. We used Matlab Simulink to build a simple model predictive control scheme. In the control simulations, the sampling time was chosen as 0.1 min and the prediction horizon was set as 10. In Fig. 2, the MI calculator computes the MI from the predicted values of operating variables based on the linear model, Eq. (30). Outputs from the MI calculator are compared with the MI set-points predefined in the operation.

Ogawa et al. [4] suggested an instantaneous MI estimation model which is based on the assumption that reaction time is much shorter than the residence time in the reactor and the typical polymer structure shares similar types [6]. Their model, which is implemented in the MI calculator shown in Fig. 2, is a linear combination of concentration ratios of each reactant and the logarithm of catalyst and temperature term and is given by

$$\log(MI_i) = \beta + a_1\frac{[H_2]}{[C_2]} + a_2\frac{[C_3]}{[C_2]} + a_3\frac{[C_4]}{[C_2]} + a_4\log[R] + a_5\log(T) \quad (33)$$

All the necessary information required in the MI calculator is supplied from the linearized process model. The main advantage of the use of the linearized process model is that we can identify other process variables as well as MIs. In the computation the unmeasured disturbances are neglected.

DISCUSSION

To check the validity of the proposed linear process model, the operation input data were fed into the process model given by Eq. (30). Practically, the MI is the only variable to be used in the comparison because only the MI is measured and used to determine the status of the product quality in actual operations. As we can see from Fig. 3, the computed MIs show acceptable tracking performance to the predefined MIs. This fact means that the proposed model can be used in the control system.

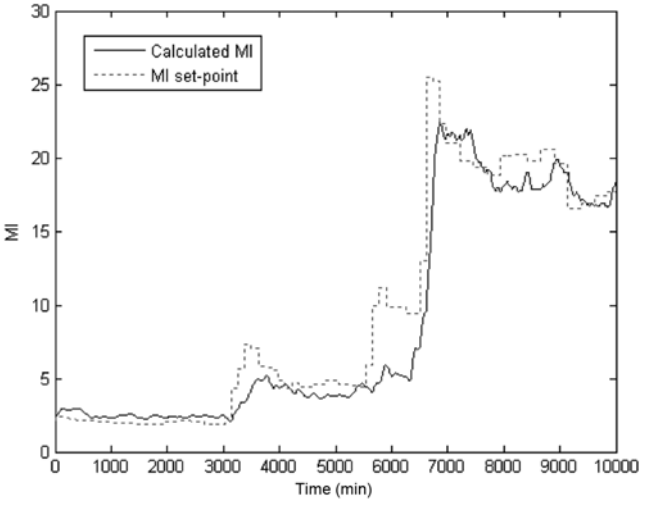

Fig. 3. Results of simulations represented in terms of MI.

Fig. 4 shows simulation results of the application of the proposed control scheme shown in Fig. 2 based on the linear process model. Fig. 4(a) shows the control performance for the staircase grade change operations. The predicted MIs using the state variables of Eq. (30) and optimal inputs computed from the proposed control scheme exhibit excellent tracking behavior. Even with the abrupt grade changes the control scheme again shows good tracking performance as shown in Fig. 4(b). When the duration of the grade change shows large variations as in Fig. 4(c), we can see satisfactory control performance again. When the desired MI changes within a small range, we have to pay close attention to meet the product specification. Even in this subtle operating situation, the proposed control scheme exhibits excellent tracking behavior in terms of MI as shown in Fig. 4(d).

CONCLUSION

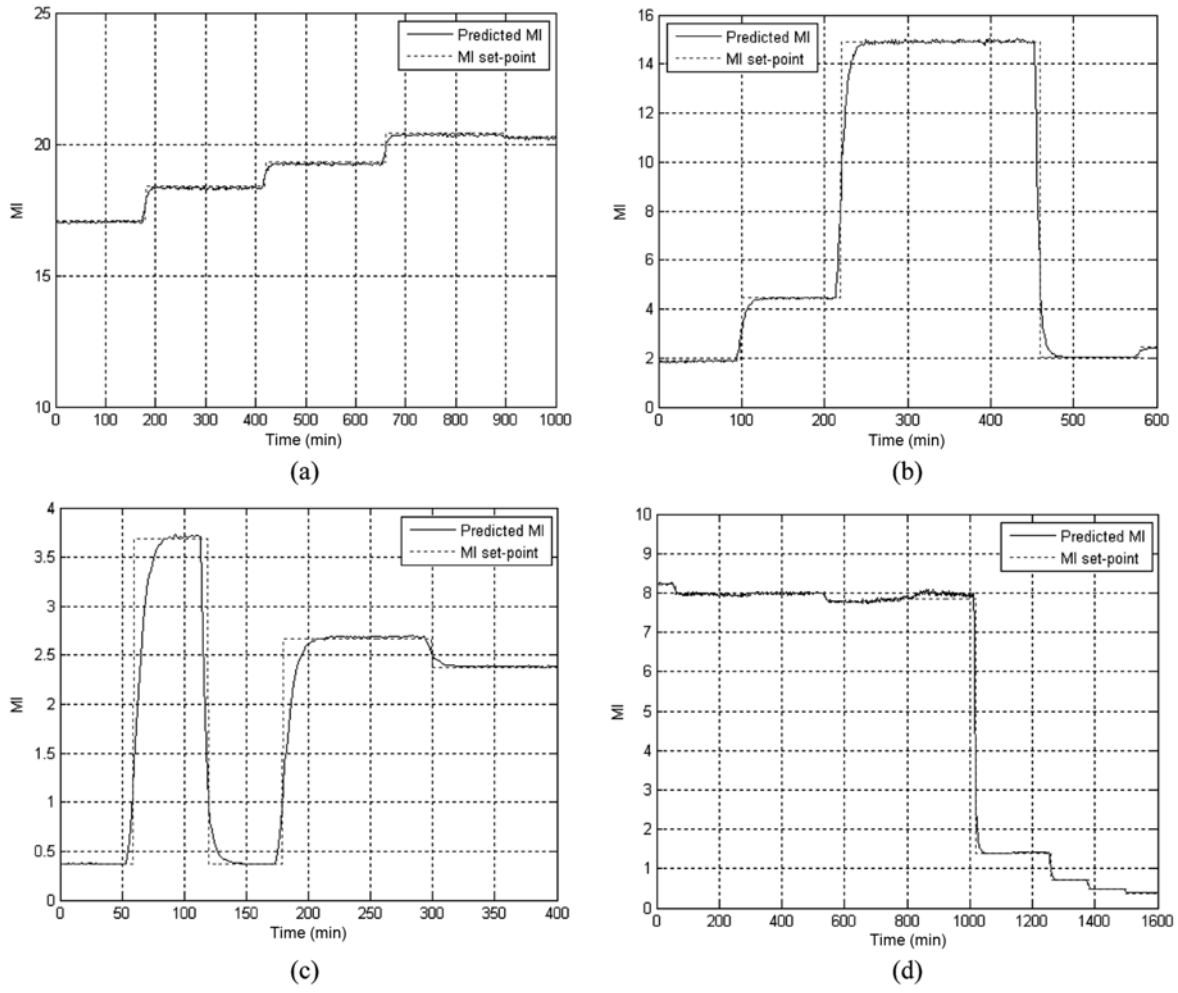

Fig. 4. Performance of the proposed control scheme in various grade change operations: (a) Staircase grade changes, (b) Abrupt grade changes, (c) Grade changes ith various duration time, (d) Grade changes within a small range.

We first investigated the model for an industrial isothermal HDPE slurry reactor. The model, consisting of several nonlinear equations, was linearized to give a linear time invariant state space model. The effectiveness of the linearized model was verified by the numerical simulations. A simple model predictive control scheme was constructed based on the linear state space model. The MI value is obtained from the values of the manipulated and controlled variables generated from the control scheme. The control performance can be evaluated from the comparison between the computed MI values and measured MI values. The control scheme showed good tracking performance in the numerical simulations. We believe that the model developed in the present study can be effectively used to predict process variables as well as to control the MI.

APPENDIX. LINEARIZATION OF THE NONLINEAR PROCESS MODEL

$$\frac{dX_1'}{dt} = F_1' + \left[-\frac{K_p A x_{3s}}{x_{5s}}\right] X_1' + \left[-\frac{K_p A (x_{1s} - MG_1)}{x_{5s}}\right] X_3' + \left[-\frac{K_p A (x_{1s} - MG_1) x_{3s}}{x_{5s}^2}\right] X_5' \tag{34}$$

$$\frac{dX_2'}{dt} = F_2' + \left[\begin{array}{c} \dfrac{-0.2268 C_v \alpha_2}{Sh\alpha_2 + (V - Sh)\left(\dfrac{K_p x_{3s}}{kL_a x_{5s}} + 1\right)} \\ \sqrt{(P - P_{out})\left(\dfrac{x_{4s}}{\rho_4 (x_{4s} + \rho_5 x_{5s})} + \dfrac{x_{5s}}{x_{4s} + \rho_5 x_{5s}}\right)} \\ -\dfrac{K_p Sh \alpha_2 x_{3s}}{x_{5s}\left(Sh\alpha_2 - (V - Sh)\left(\dfrac{K_p x_{3s}}{kL_a x_{5s}} + 1\right)\right)} \end{array}\right] X_2'$$

$$+ \left[\begin{array}{c} \dfrac{0.2268 C_v (V - Sh)\dfrac{K_p}{kL_a x_{5s}}}{\left[Sh\alpha_2 + (V - Sh)\left(\dfrac{K_p x_{3s}}{kL_a x_{5s}} + 1\right)\right]} \\ \sqrt{(P - P_{out})\left(\dfrac{x_{4s}}{\rho_4 (x_{4s} + \rho_5 x_{5s})} + \dfrac{x_{5s}}{x_{4s} + \rho_5 x_{5s}}\right)} \\ K_p Sh \alpha_2 x_{2s} x_{5s}\left(Sh\alpha_2 - (V - Sh)\left(\dfrac{K_p x_{3s}}{kL_a x_{5s}} + 1\right)\right) \\ -\dfrac{+ (V - Sh)\dfrac{K_p^2 Sh \alpha_2 x_{3s}}{kL_a}}{x_{5s}^2\left(Sh\alpha_2 + (V - Sh)\left(\dfrac{K_p x_{3s}}{kL_a x_{5s}} + 1\right)\right)^2} \end{array}\right] X_3'$$

$$+\left[\begin{array}{l}\dfrac{-0.2268C_v\alpha_2x_{2s}}{Sh\alpha_2+(V-Sh)\left(\dfrac{K_px_{3s}}{kL_ax_{5s}}+1\right)}\\ *0.5_{-1}\sqrt{(P-P_{out})\left(\dfrac{x_{4s}}{\rho_4(x_{4s}+\rho_5x_{5s})}+\dfrac{x_{5s}}{x_{4s}+\rho_5x_5}\right)}\\ *(P-P_{out})\left(\dfrac{x_{4s}+\rho_5x_{5s}}{\rho_4(x_{4s}+\rho_5x_{5s})^2}-\dfrac{x_{5s}}{(x_{4s}+\rho_5x_5)^2}\right)\end{array}\right]X'_4$$

$$+\left[\begin{array}{l}-0.2268C_v\sqrt{(P-P_{out})\left(\dfrac{x_{4s}}{\rho_4(x_{4s}+\rho_5x_{5s})}+\dfrac{x_{5s}}{x_{4s}+\rho_5x_5}\right)}\\ \dfrac{-(V-Sh)\dfrac{K_p\alpha_2x_{2s}x_{3s}}{kL_a}}{\left[Sh\alpha_2+(V-Sh)\left(\dfrac{K_px_{3s}}{kL_ax_{5s}}+1\right)\right]^2}-\dfrac{0.2268C_v\alpha_2x_{2s}}{Sh\alpha_2+(V-Sh)\left(\dfrac{K_px_{3s}}{kL_ax_{5s}}+1\right)}\\ *0.5_{-1}\sqrt{(P-P_{out})\left(\dfrac{-\rho_4\rho_5}{\rho_4^2(x_{4s}+\rho_5x_{5s})^2}+\dfrac{x_{4s}}{x_{4s}+\rho_5x_5}\right)}\\ *(P-P_{out})\left(\dfrac{-\rho_5x_{4s}}{\rho_4(x_{4s}+\rho_5x_{5s})^2}-\dfrac{x_{4s}}{(x_{4s}+\rho_5x_5)^2}\right)\\ +\dfrac{\left(Sh\alpha_2-(V-Sh)\left(\dfrac{K_px_{3s}}{kL_ax_{5s}}+1\right)\right)-\dfrac{K_pkL_a(V-Sh)x_{3s}x_{5s}}{kL_a^2x_{5s}^2}}{x_{5s}^2\left(Sh\alpha_2-(V-Sh)\left(\dfrac{K_px_{3s}}{kL_ax_{5s}}+1\right)\right)^2}\end{array}\right]X'_5 \quad (35)$$

$$\frac{dX'_3}{dt}=F'_3+\left[\frac{-0.2268C_v}{Sh}\sqrt{(P-P_{out})\left(\frac{x_s}{\rho_4(x_{4s}+\rho_5x_{5s})}+\frac{x_{5s}}{x_{4s}+\rho_5x_5}\right)}\right]X'_3$$

$$+\left[\begin{array}{l}\dfrac{-0.2268C_vx_{3s}}{Sh}*0.5\left((P-P_{out})\left(\dfrac{x_{4s}}{\rho_4(x_{4s}+\rho_5x_{5s})}+\dfrac{x_{5s}}{x_{4s}+\rho_5x_5}\right)\right)^{-0.5}\\ *(P-P_{out})\left(\dfrac{\rho_5x_{5s}}{\rho_4(x_{4s}+\rho_5x_{5s})^2}+\dfrac{x_{5s}}{(x_{4s}+\rho_5x_5)^2}\right)\end{array}\right]X'_4$$

$$+\left[\begin{array}{l}\dfrac{-0.2268C_vx_{3s}}{Sh}*0.5\left((P-P_{out})\left(\dfrac{x_{4s}}{\rho_4(x_{4s}+\rho_5x_{5s})}+\dfrac{x_{5s}}{x_{4s}+\rho_5x_5}\right)\right)^{-0.5}\\ *(P-P_{out})\left(\dfrac{-\rho_5x_{4s}}{\rho_4(x_{4s}+\rho_5x_{5s})^2}+\dfrac{x_{4s}}{(x_{4s}+\rho_5x_5)^2}\right)\end{array}\right]X'_5 \quad (36)$$

$$\frac{dX'_4}{dt}=F'_4+\left[\frac{56}{1000}\frac{K_px_{3s}}{x_{5s}}\frac{\alpha_2Sh}{\alpha_2Sh-(V-Sh)\left(\dfrac{K_px_{3s}}{kL_ax_{5s}}+1\right)}\right]X'_2$$

$$+\left[\begin{array}{l}\dfrac{56K_p\alpha_2Shx_{2s}*1000x_{5s}\left(\left(\alpha_2Sh-(V-Sh)\left(\dfrac{K_px_{3s}}{kL_ax_{5s}}+1\right)\right)\right.}{\left.+\dfrac{K_px_{3s}(V-Sh)}{kL_ax_{5s}}\right)}\\ \left(1000\alpha_2Shx_{5s}-(V-Sh)\left(\dfrac{K_px_{3s}}{kL_ax_{5s}}+1\right)\right)^2\end{array}\right]X'_3$$

$$+[-0.2268C_v$$

$$\left\{\begin{array}{l}\dfrac{1}{Sh}\sqrt{(P-P_{out})\left(\dfrac{x_{4s}}{\rho_4(x_{4s}+\rho_5x_{5s})}+\dfrac{x_{5s}}{x_{4s}+\rho_5x_5}\right)}\\ +\dfrac{0.5x_{4s}}{Sh}\left((P-P_{out})\left(\dfrac{x_{4s}}{\rho_4(x_{4s}+\rho_5x_{5s})}+\dfrac{x_{5s}}{x_{4s}+\rho_5x_5}\right)\right)^{-0.5}\\ *(P-P_{out})\left(\dfrac{\rho_5x_{5s}}{\rho_4(x_{4s}+\rho_5x_{5s})^2}-\dfrac{x_{5s}}{(x_{4s}+\rho_5x_5)^2}\right)\end{array}\right\}\Bigg]X'_4$$

$$+\left[\begin{array}{l}-0.2268C_v\dfrac{0.5x_{4s}}{Sh}\left((P-P_{out})\left(\dfrac{x_{4s}}{\rho_4(x_{4s}+\rho_5x_{5s})}+\dfrac{x_{5s}}{x_{4s}+\rho_5x_5}\right)\right)^{-0.5}\\ *(P-P_{out})\left(\dfrac{-\rho_5x_{4s}}{\rho_4(x_{4s}+\rho_5x_{5s})^2}-\dfrac{x_{4s}}{(x_{4s}+\rho_5x_5)^2}\right)\\ -\left(\begin{array}{l}\alpha_2Sh-(V-Sh)\left(\dfrac{K_px_{3s}}{kL_ax_{5s}}+1\right)\\ +\dfrac{K_px_{3s}(V-Sh)}{kL_ax_{5s}}\end{array}\right)K_p\alpha_2Shx_{2s}x_{3s}\\ +\dfrac{56}{1000}\dfrac{}{x_{5s}\left(\alpha_2Sh-(V-Sh)\left(\dfrac{K_px_{3s}}{kL_ax_{5s}}+1\right)\right)^2}\end{array}\right]X'_5 \quad (37)$$

$$\frac{dX'_5}{dt}=F'_5$$

$$+\left[\begin{array}{l}\dfrac{-0.2268C_v}{2}\left((P-P_{out})\left(\dfrac{x_{4s}}{\rho_4(x_{4s}+\rho_5x_{5s})}+\dfrac{x_{5s}}{x_{4s}+\rho_5x_5}\right)\right)^{-0.5}\\ *(P-P_{out})\left(\dfrac{\rho_5x_{5s}}{\rho_4^2(x_{4s}+\rho_5x_{5s})^2}-\dfrac{x_{5s}}{(x_{4s}+\rho_5x_5)^2}\right)\left(\dfrac{x_{4s}/\rho_4+x_{5s}}{x_{4s}}-\dfrac{1}{\rho_4}\right)\\ +0.2268C_v\left(\dfrac{x_{5s}}{x_{4s}^2}\right)\sqrt{(P-P_{out})\left(\dfrac{x_{4s}}{\rho_4(x_{4s}+\rho_5x_{5s})}+\dfrac{x_{5s}}{x_{4s}+\rho_5x_5}\right)}\end{array}\right]X'_4$$

$$+\left[\begin{array}{l}\dfrac{-0.2268C_v}{2}\left((P-P_{out})\left(\dfrac{x_{4s}}{\rho_4(x_{4s}+\rho_5x_{5s})}+\dfrac{x_{5s}}{x_{4s}+\rho_5x_5}\right)\right)^{-0.5}\\ *(P-P_{out})\left(\dfrac{-\rho_5x_{4s}}{\rho_4^2(x_{4s}+\rho_5x_{5s})^2}-\dfrac{x_{4s}}{(x_{4s}+\rho_5x_5)^2}\right)\left(\dfrac{x_{4s}/\rho_4+x_{5s}}{x_{4s}}-\dfrac{1}{\rho_4}\right)\\ -0.2268C_v\left(\dfrac{1}{x_{4s}}\right)\sqrt{(P-P_{out})\left(\dfrac{x_{4s}}{\rho_4(x_{4s}+\rho_5x_{5s})}+\dfrac{x_{5s}}{x_{4s}+\rho_5x_5}\right)}\end{array}\right]X'_5 \quad (38)$$

NOMENCLATURE

ACT : reciprocal of average chain length [-]
C_v : valve coefficient [-]
F_1 : flow-rate of hydrogen in feed [kmol/h]
F_2 : flow-rate of ethylene in feed [kmol/h]
F_3 : flow-rate of catalyst in feed [mol/h]
F_4 : flow-rate of comonomer in feed [t/h]
F_5 : flow-rate of hexane in feed [m^3/h]
G_1 : output flow-rate of hydrogen in gas model [kg/h]
G_2 : output flow-rate of ethylene in gas model [kg/h]
G : density of slurry [t/m^3]
H : height of reactor [m]
K_p : propagation rate constant [m^3/mol/h]
kL_a : mass transfer coefficient for ethylene [1/h]

L_1 : output flow-rate of hydrogen in slurry model [kmol/h]
L_2 : output flow-rate of ethylene in slurry model [kmol/h]
L_3 : output flow-rate of catalyst in slurry model [mol/h]
L_4 : output flow-rate of comonomer in slurry model [t/h]
L_5 : output flow-rate of hexane in slurry model [m^3/h]
MI_i, MI_{inst} : instantaneous MI [g/10 min]
MG_1 : amount of hydrogen in gas phase [kmol]
MG_2 : amount of ethylene in gas phase [kmol]
ML_1 : amount of hydrogen in slurry [kmol]
ML_2 : amount of ethylene in slurry [kmol]
P : pressure [atm or psi]
P_{out} : outlet pressure [atm]
Q : ratio of hydrogen to ethylene [-]
R : gas constant [m^3 atm/kmol/K]
r_1 : rate of consumption of hydrogen [kmol/h]
r_1 : rate of consumption of ethylene [kmol/h]
S : area of reactor [m^2]
T : temperature [K]
V : volume of the reactor [m^3]
x_1 : amount of hydrogen in reactor [kmol]
x_2 : amount of ethylene in reactor [kmol]
x_3 : amount of catalyst in slurry [mol]
x_4 : amount of comonomer in slurry [t]
x_5 : amount of hexane in slurry [m^3]

Greek Letters

α_1 : reciprocal of Henry's constant for hydrogen [-]
α_2 : reciprocal of Henry's constant for ethylene [-]
η : solubility efficiency [-]
ρ_4 : density of comonomer [t/m^3]
ρ_5 : density of hexane [t/m^3]

REFERENCES

1. K. B. McAuley and J. F. MacGregor, *AIChE J.*, **37**, 825 (1991).
2. K. B. McAuley and J. F. MacGregor, *AIChE J.*, **38**, 1564 (1992).
3. K. B. McAuley and J. F. MacGregor, *AIChE J.*, **39**, 855 (1993).
4. M. Ogawa, M. Ohshima, K. Morinaga and F. Watanabe, *Journal of Process Control*, **9**, 51 (1999).
5. M. M. Kannan and J. Shubhangi, *Chemical Engineering Science*, **56**, 3611 (2001).
6. M. Oshima and T. Masataka, *Journal of Process Control*, **10**, 135 (2000).